

## **SPATIAL DIFFERENTIATION IN ABSORBED SOLAR RADIATION IN THE OJCÓW NATIONAL PARK**

**Jakub Wojkowski, Barbara Skowera**

Department of Ecology, Climatology and Pollution of the Air  
Agricultural University in Kraków, Poland

### **Abstract**

The research presents the analysis of spatial variations of absorbed solar radiation in the Ojców National Park in the south part of Krakowsko-Częstochowska Upland in Poland. This area is characterized by varied diverse relief. The solar radiation budget was estimated on the basis of multispectral satellite images and the solar radiation model implemented to the Geographical Information Systems (GIS). The materials used in the research were digital terrain model (DTM) with spatial resolution of 20 m/pixel and multispectral satellite images LANDSAT-7. The digital terrain model was used to mark indispensable topography parameters like elevation, slope, aspect and sky factor. The modelling was realized in a few stages. During the first stage the spatial data base for the tested area was prepared. During the second one the flux of global solar radiation was calculated. On the basis of the satellite images LANDSAT-7 the value of surface albedo  $\alpha$  was calculated.

It was found that in the case of the Ojców National Park, highly diverse relief seems to be the main factor influencing controlling the values of absorbed solar radiation. The solar radiation budget is also dependent on the albedo. Despite a considerable diversity of land cover and land use in the Ojców National Park, the impact of albedo on absorbed solar radiation value is decidedly less significant than the relief.

### **INTRODUCTION**

Solar radiation absorbed by the Earth  $K^*$  is the difference between global solar radiation  $K_{\downarrow}$  and reflected solar radiation  $K_{\uparrow}$ . It plays an important role in shaping the climate conditions of the relevant area as it influences the energetic balance and at the same time thermal and humidity conditions of atmosphere surface layers and its base (Paszyński at all 1999). Therefore, it is very important to learn the components of surface radiation balance and its structure.

The studies of components of radiation balance in the Ojców National Park (OPN) was begun by J. Klein (1974, 1992). Dynamic development of remote sensing and the increase in the number of satellites has created new quality in climatic research. It has become possible to conduct detailed research on spatial variability of some climate components for a larger area thanks to satellite images. The research of satellite climatology prepared on high resolution satellite images the OPN have been connected with spatial diversity of global solar radiation (Wojkowski 2006) and the brightness surface temperature (Wojkowski 2007a) as well as the vegetation index NDVI (Wojkowski 2007b). The aim of the research was the recognition of absorbed solar radiation during the year and drawing up a map of its spatial distribution in the OPN.

### **METHOD**

To analyze spatial diversity of absorbed solar radiation on the area of the OPN digital elevation model – DEM (WODGiK) and high resolution multispectral satellite images Landsat 7 were used. Diagram of absorbed solar radiation is shown at figure 1.

In the first stage the map of land use and cover for the area of the OPN was prepared. The satellite images of Landsat 7 underwent the supervised classification. There were seven classes specified while preparing the map of cover and use: urban area, grassland, cultivated fields, broadleaved forest, coniferous forest, mixed forest and waters (fig. 2). Percentage part of particular classes of land cover and use in the total area of the examined area is shown in table 1.

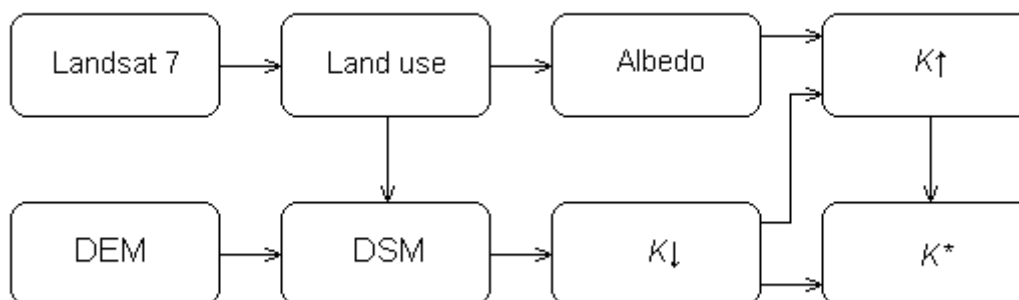


Fig. 1. Diagram of absorbed solar radiation calculating  $K^*$

Then in order to calculate the albedo, satellite images Landsat7 were used. Radiation recorded by scanner ETM+ (Enhanced Thematic Mapper Plus) in panchromatic spectral band (0,52 do 0,90  $\mu\text{m}$ ) was used to calculate the value of albedo with the spatial resolution 15  $\text{m}\cdot\text{pixel}^{-1}$  (Irish 2000).

Table 1. The percentage of land use and land cover classes in the whole study area

Land use and land cover classes	%
urban area	6,15
grassland	16,13
cultivated fields	45,02
broadleaved forest	13,71
coniferous forest	4,12
mixed forest	14,55
waters	0,32
sum	100,00

35 satellite images from the period 09.08.1999 - 21.09.2009 have been analyzed. On their basis monthly values of albedo for particular cover and use classes of the OPN were prepared. For the winter months the value of albedo was dependent on the snow cover (tab. 2) and was calculated according to the below equation:

$$\alpha_m = \alpha_{ps} \frac{LD_{ps}}{LD_m} + \alpha_{bs} \frac{LD_{bs}}{LD_m}$$

where:

$\alpha_m$  – monthly mean albedo value for the given month

$\alpha_{ps}$  – albedo value in the given month read from satellite images on which snow cover was recorded

$\alpha_{bs}$  – albedo value in the given month read from satellite images without snow cover

$LD_{ps}$  – mean number of days with snow cover in the given month

$LD_{bs}$  – mean number of days without snow cover in the given month

$LD_m$  – number of days in the given month

Table 2. Mean number of days with snow cover  $LD_{ps}$  in the OPN (1991-2010)

I	II	III	IV	V	VI	VII	VIII	IX	X	XI	XII	Year
25	22	14	3	0	0	0	0	0	0	7	20	91

The albedo for different surface classes in the particular months was the basis for calculating the mean albedo value during the year for the whole examined area. (tab. 3).

$$\alpha_{sr} = \frac{\sum_{i=1}^n \alpha_i P_i}{\sum_{i=1}^n P_i}$$

where:

$\alpha_{sr}$  – mean area albedo value for the OPN

$\alpha_i$  – albedo value for the given cover and use class the OPN

$P_i$  – area of the given cover and use class OPN

The results of analysis of spectral satellite images and above calculations are presented in table 3.

Table 3. Monthly value of albedo of land use and land cover surface in OPN on the basis of satellite images

Land use and land cover classes	I	II	III	IV	V	VI	VII	VIII	IX	X	XI	XII	Year
urban area	0,13	0,13	0,12	0,12	0,13	0,13	0,13	0,13	0,12	0,12	0,12	0,12	0,13
grassland	0,31	0,30	0,24	0,18	0,18	0,19	0,20	0,20	0,18	0,16	0,17	0,26	0,21
cultivated fields	0,31	0,31	0,24	0,19	0,19	0,20	0,21	0,21	0,19	0,17	0,18	0,26	0,22
broadleaved forest	0,10	0,10	0,09	0,12	0,14	0,17	0,17	0,17	0,16	0,15	0,12	0,09	0,13
coniferous forest	0,10	0,10	0,10	0,11	0,12	0,13	0,13	0,13	0,12	0,11	0,10	0,09	0,11
mixed forest	0,11	0,11	0,10	0,12	0,13	0,15	0,15	0,15	0,14	0,12	0,10	0,10	0,12
waters	0,19	0,19	0,15	0,09	0,08	0,08	0,08	0,08	0,08	0,09	0,09	0,16	0,11
$\alpha_{sr}$	0,23	0,23	0,19	0,16	0,17	0,18	0,18	0,18	0,17	0,15	0,15	0,20	0,18

Mean monthly albedo values were assigned to particular map classes of cover and use (fig. 2). The spatial albedo arrangement was obtained in the OPN in particular months and during the year with the spatial with the spatial resolution  $15 \text{ m} \cdot \text{pixel}^{-1}$  (fig. 3).

The next stage was to transform DEM to digital surface model (DSM) which represents the earth's surface and includes all objects on it. The map of land cover and use (fig. 3), which had been prepared earlier, was used here. Digital surface model is the surface on which global solar radiation comes  $K_{\downarrow}$ .

The following stage was calculating global solar radiation  $K_{\downarrow}$  on the area of the OPN. The algorithm by Rich (1994) was used. The algorithm is based on the Bouguer-Lambert's law describing the extinction of solar radiation in the atmosphere and uses DSM to calculate components of topography like horizon obstruction, aspect, slope and elevation. The calculating of solar radiation was done for the particular months of the year and the annual sum  $K_{\downarrow}$  with the spatial resolution  $20 \text{ m} \cdot \text{pixel}^{-1}$  (fig. 4).

According to the calculated albedo (fig. 3) and calculated global solar radiation  $K_{\downarrow}$  (fig. 4) reflected solar radiation  $K_{\uparrow}$  was counted as follows:

$$K_{\uparrow} = \alpha \cdot K_{\downarrow}$$

where:

$K_{\uparrow}$  – reflected solar radiation

$K_{\downarrow}$  – global solar radiation  
 $\alpha$  – albedo

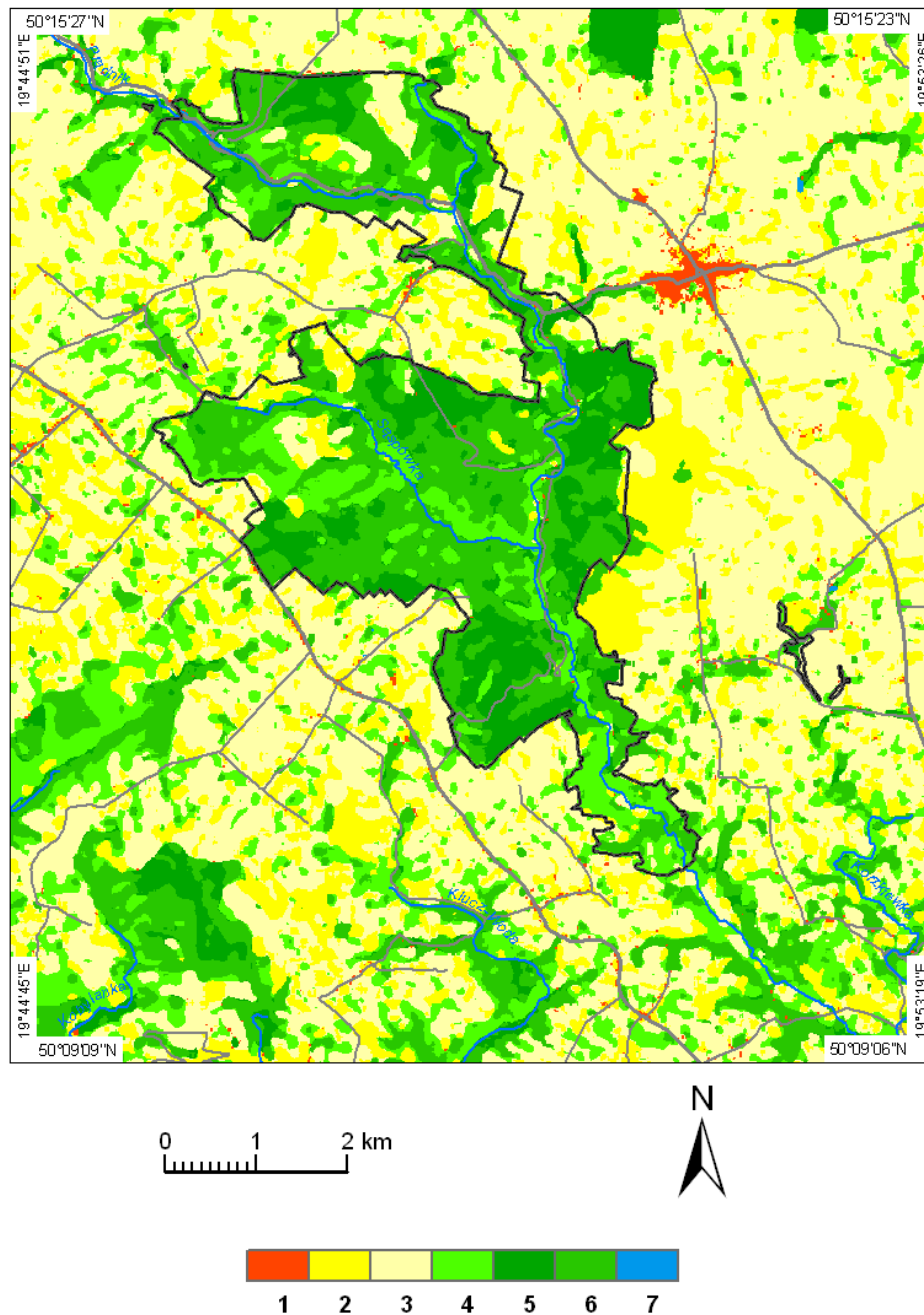


Fig. 2. Map of land use and land cover of the OPN: 1- urban area, 2 - grassland, 3 - cultivated fields, 4 - broadleaved forest, 5- coniferous forest, 6 - mixed forest, 7 - waters

The result of the calculations was a map of spatial diversity of annual sum  $K_{\uparrow}$  presented in figure 5.

Absorbed solar radiation  $K^*$  is the difference between  $K_{\downarrow}$  and  $K_{\uparrow}$ . It was counted as follows:

$$K^* = K_{\downarrow} - K_{\uparrow}$$

where:

$K^*$  – absorbed solar radiation  
 $K_{\downarrow}$  – global solar radiation  
 $K_{\uparrow}$  – reflected solar radiation

Spatial distribution of the annual sum  $K^*$  is shown in figure 6.

All the spatial and spectral analysis and calculating  $K_{\downarrow}$ ,  $\alpha$ ,  $K_{\uparrow}$  i  $K^*$  was prepared with the use of GIS. The research covered the area of OPN with the extent of longitude 50°09'06"N and 50°15'27"N and latitude 19°44'45"E and 19°53'26"E.

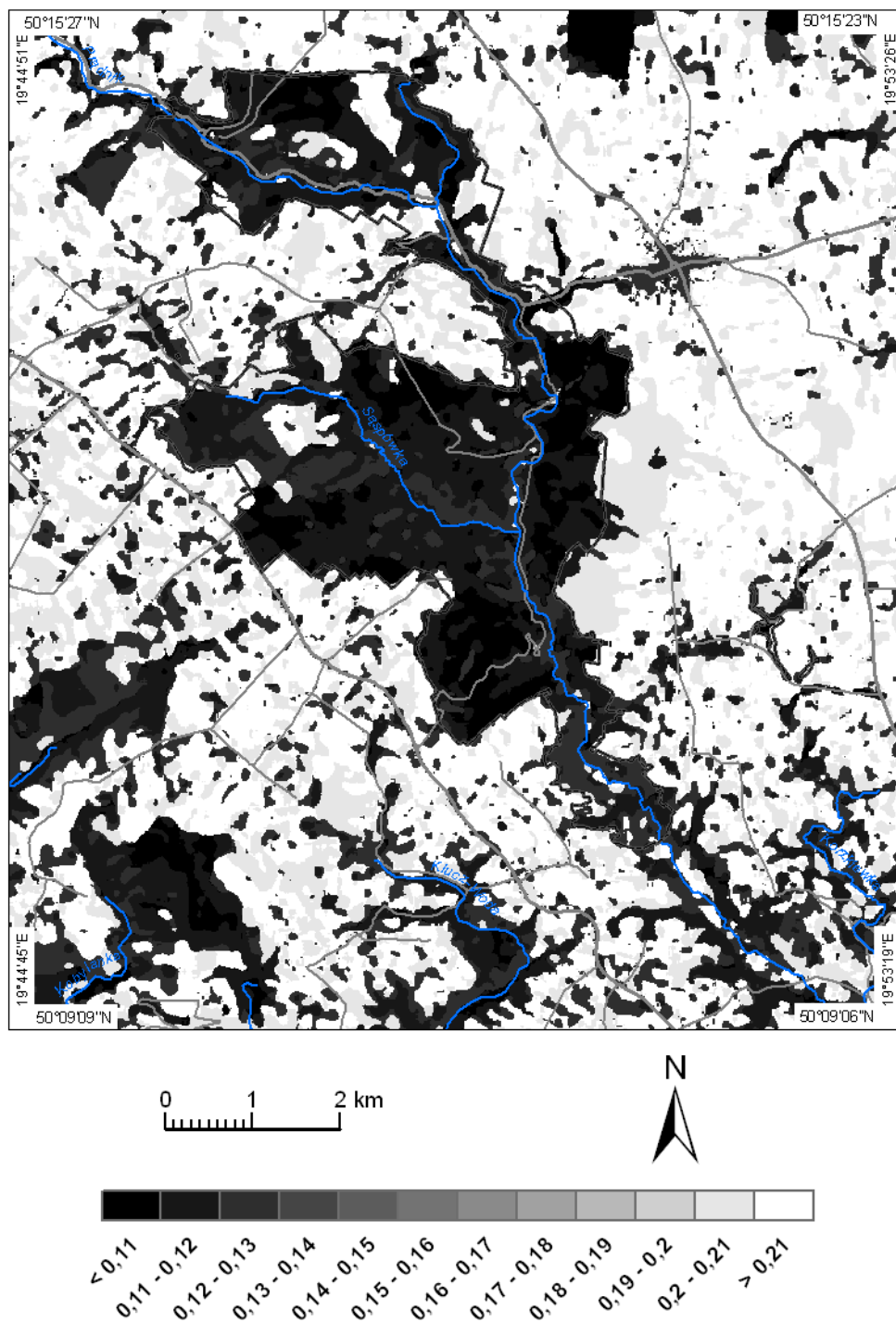


Fig. 3. Annual albedo  $\alpha$  in the OPN

## RESULTS

The climate conditions of the OPN are formed by the quantity of energy coming to the surface and the way it is used in various physical processes. The absorbed solar radiation is the main component in the heat balance equation which is transformed into heat. The value  $K^*$  depends on the same factors which influence the global and reflected solar radiation. Diverse relief and land cover of the OPN make spatial diversity significant that can be observed in the maps of calculated spatial distribution of the  $K_{\downarrow}$ ,  $\alpha$ ,  $K_{\uparrow}$  i  $K^*$  (fig. 3, 4, 5 and 6).

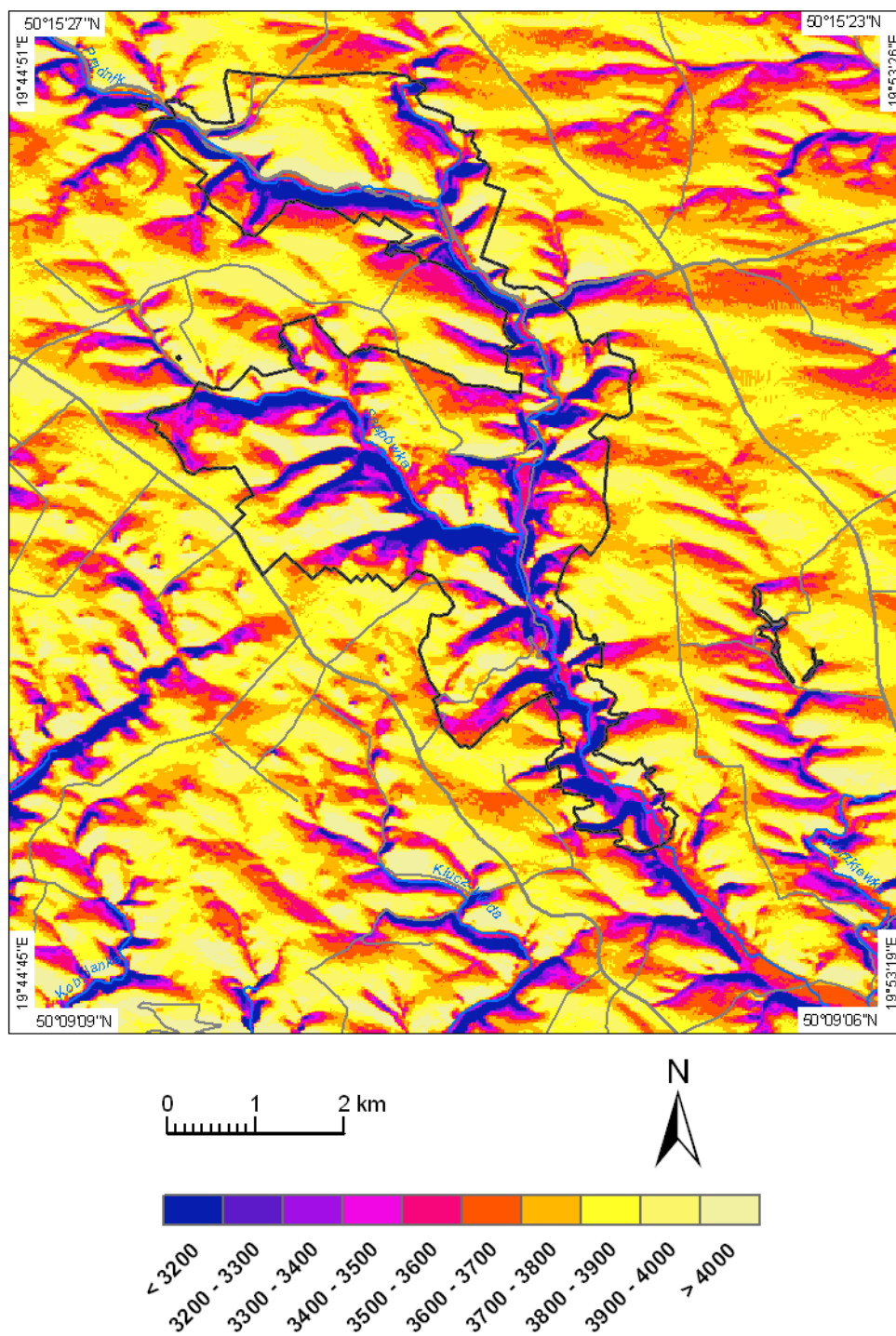


Fig. 4. Annual global solar radiation  $K_{\downarrow}$  [ $\text{MJ}\cdot\text{m}^{-2}$ ] in the OPN



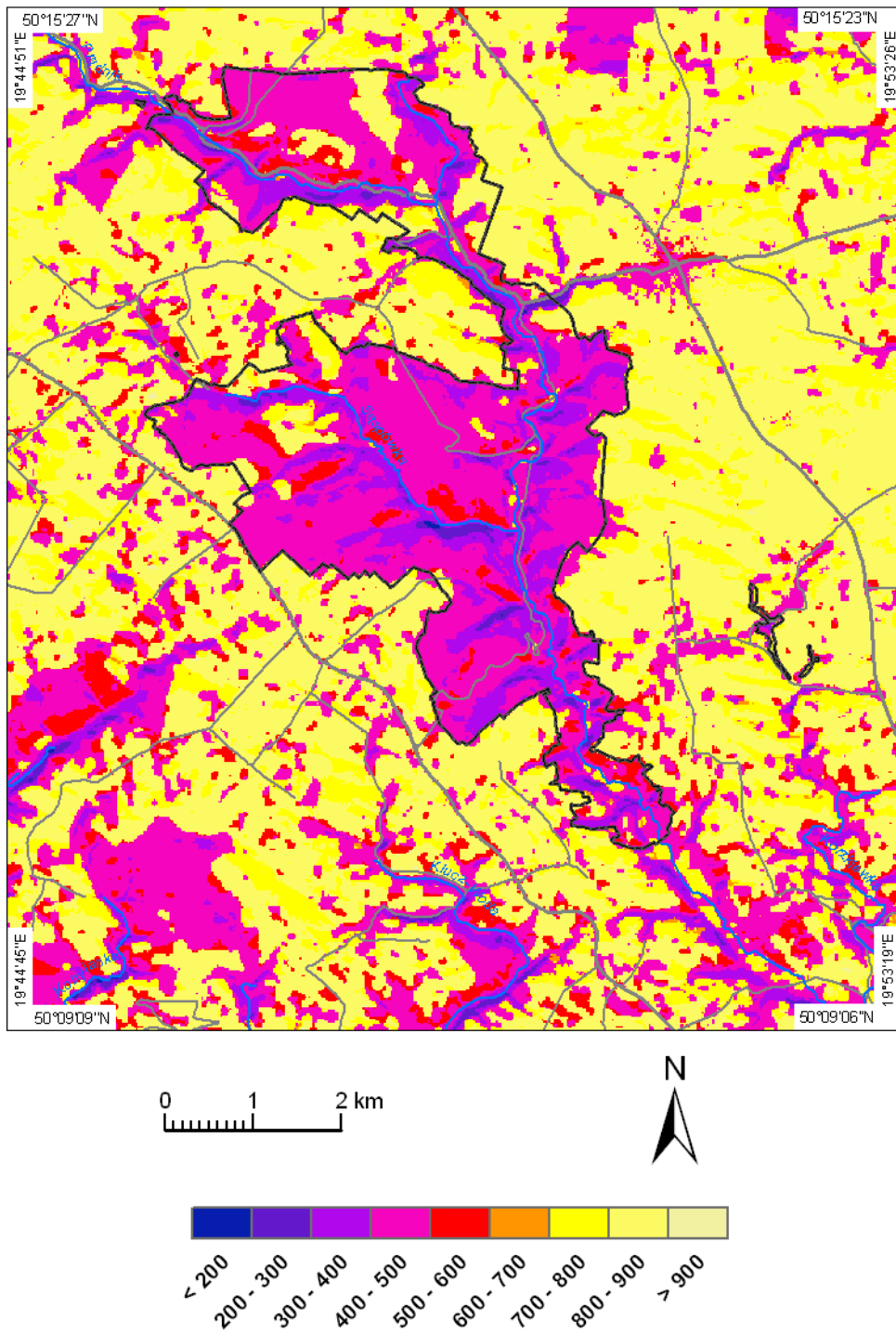


Fig. 5. Annual reflected solar radiation  $K_{\uparrow}$  [ $\text{MJ}\cdot\text{m}^{-2}$ ] in the OPN

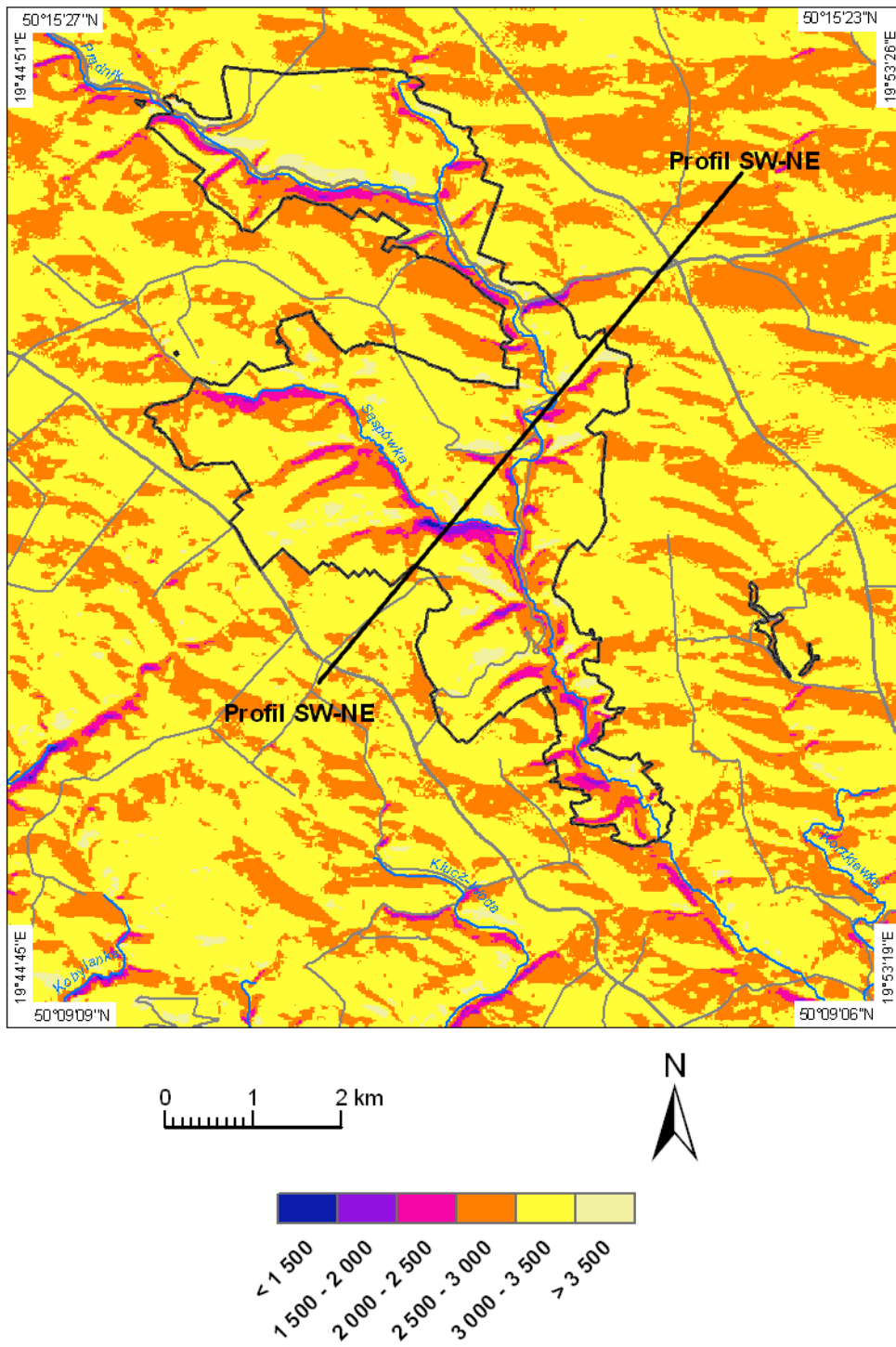


Fig. 6. Annual absorbed solar radiation  $K^*$  [ $\text{MJ}\cdot\text{m}^{-2}$ ] in the OPN



The results of the calculated components of the solar radiation balance during the year is shown in table 4.

Table 4. Calculated monthly value of global  $K_{\downarrow}$ , reflected  $K_{\uparrow}$  and absorbed  $K^*$  solar radiation in  $[MJ\cdot m^{-2}]$  in OPN

Components of the solar radiation balance		I	II	III	IV	V	VI	VII	VIII	IX	X	XI	XII	Year
$K_{\downarrow}$	min	11	24	60	113	206	242	223	139	67	33	11	6	1177
	max	104	175	365	500	632	659	647	553	406	234	107	68	4348
	mean	60	107	271	429	584	620	604	488	312	152	59	35	3721
$K_{\uparrow}$	min	1	3	6	14	27	36	33	21	8	4	1	1	141
	max	32	52	88	93	119	132	135	115	73	37	18	18	942
	mean	14	25	51	69	97	112	113	91	53	23	9	7	677
$K^*$	min	9	20	54	99	179	206	189	118	58	29	10	5	1016
	max	88	151	326	440	547	580	567	472	343	197	89	57	3750
	mean	45	82	221	360	487	506	491	397	259	129	50	28	3055

The calculated values show that during the year the area of the OPN gets the average  $3721 MJ\cdot m^{-2}$  of solar energy,  $677 MJ\cdot m^{-2}$  of that it reflects and  $3055 MJ\cdot m^{-2}$  is absorbed by the area (fig4). The lowest sums of the balance components occur in November, December and January and then they get higher until summer months. Then they get smaller until December. The mean monthly  $K^*$  equals  $28 MJ\cdot m^{-2}$  in December, which is only 1% of the annual sum. The highest monthly  $K^*$  occurs in June and amounts to  $506 MJ\cdot m^{-2}$  (17% of the annual sum). Summer months are characterized by the biggest spatial distribution of solar absorbed radiation sum. Only in June and July it is 33% of the annual sum. From May to August it is almost 62% of the annual sum  $K^*$  while from November to February it is merely 7% of the sum.

The lowest values of absorbed solar radiation in the OPN occur at the bottoms of deep valleys, canyons and low situated horizon obstructed slopes with northern aspect. It was observed that the lowest annual sum of absorbed solar radiation ( $1016 MJ\cdot m^{-2}$ ) occurred on a steep slope covered with forest, with the inclination of  $56^{\circ}$  and north-east aspect. It is 376 m above sea level and is situated at the entrance of Jamki Canyon in Sąspowska Valley ( $19^{\circ}48'53,76''E$ ,  $50^{\circ}12'13,79''N$ ). The lowest annual sum of global solar radiation  $K_{\downarrow}$  ( $1117 MJ\cdot m^{-2}$ ) for the OPN also was recorded in the same place.

The highest values of the absorbed solar radiation occur on hilltops, which means in places characterized by insignificant horizon obstruction and on slopes with southern aspects. The highest values of the absorbed solar radiation in the OPN was observed in the very sunny place for which annual sum of the absorbed solar radiation  $K^*$  is  $3750 MJ\cdot m^{-2}$  and global solar radiation  $K_{\downarrow}$  is  $4348 MJ\cdot m^{-2}$ . It is the part of Chelmowa Mountain covered with forest (461 m above sea level) with the inclination  $30^{\circ}$  to the south ( $19^{\circ}49'22,73''E$ ,  $50^{\circ}11'56,74''N$ ).

The differences in spatial distribution of absorbed solar radiation described above, are clearly seen on the profile SW-NE (fig. 7). The profile was led through different kinds of land cover. It goes from south-west towards north-east (fig. 6). Value diversity of the balance components  $K_{\downarrow}$ ,  $K_{\uparrow}$  i  $K^*$  can be seen on the profile, they are connected with insolation conditions and different way of land use and land cover. The biggest differences are observed at the point where the profile lines cross the valleys. It results from the fact that solar radiation is higher at the hilltops than at the valley bottoms. The smallest differences of absorbed solar radiation  $K^*$  in the profile SW-NE occur on cultivated fields and green areas in Czajowice. This is a flat area with insignificant horizon obstruction, homogenous land cover and high albedo.

## SUMMARY

The research of spatial distribution of solar balance radiation showed its significant spatial diversity in the OPN. Because of varied relief, diverse morphological forms, aspect and slope, denivelation and diversity of land cover and land use there is high diversity of solar conditions.

According to the research the annual sums of absorbed solar radiation  $K^*$  are between 1016 MJ·m<sup>-2</sup> and 3750 MJ·m<sup>-2</sup>. They make up about 82% of the annual sum of global solar radiation  $K_{\downarrow}$ .

The spatial distribution of absorbed solar radiation  $K^*$  depends mainly on the factors which create insolation conditions such as: elevation, aspect, slope and horizon obstruction. In the OPN varied relief seems to be the main factor creating absorbed solar radiation  $K^*$ .

Absorbed solar radiation  $K^*$  depends also on the reflecting power of a surface. In the OPN the varied relief has much bigger influence on the absorbed solar radiation  $K^*$  than the varied land cover and land use (albedo).

## Bibliography

- Irish R.R., 2000, Landsat 7 science data user's handbook, Report 430-15-01-003-0, National Aeronautics and Space Administration.
- Klein, J. 1974: Mezo- i mikroklimat Ojcowskiego Parku Narodowego. *Studia Naturae A* (8): 1–105.
- Klein, J. 1992: Radiational climatic factors and evaporation in the Ojców National Park. *Prądnik. Prace Muz. Szafera* 5: 29–34.
- Paszyński J, Skoczek J., Miara K., 1999. Wymiana energii między atmosferą a podłożem jako podstawa kartowania topoklimatycznego. *Dokumentacja Geograficzna* nr 14. PAN IGiPZ, Warszawa.
- Rich P.M. 1994, Using viewshed models to calculate intercepted solar radiation: applications in ecology. *American Society for Photogrammetry and Remote. Sensing Technical Papers*.
- WODGiK, Digital elevation model of the Ojców National Park with the spatial resolution 20 m·pixel<sup>-1</sup>, Wojewódzki Ośrodek Dokumentacji Geodezyjnej i Kartograficznej w Krakowie.
- Wojkowski J. 2006. The solar radiation modeling using GIS in the Ojców National Park. „*Ann.UMCS*”, Sectio B (LXI [61]): 468–477.
- Wojkowski J., 2007a: The radiation budget modeling using GIS and satellite images. *Pamiętnik Puławski*, Z. 144, p. 155-167, Puławy.
- Wojkowski J., 2007b: Usage of multispectral Terra ASTER satellite images in research of land surface temperature. *Acta Agrophysica* 9(3), Vol. 148, Lublin, s. 791-807.

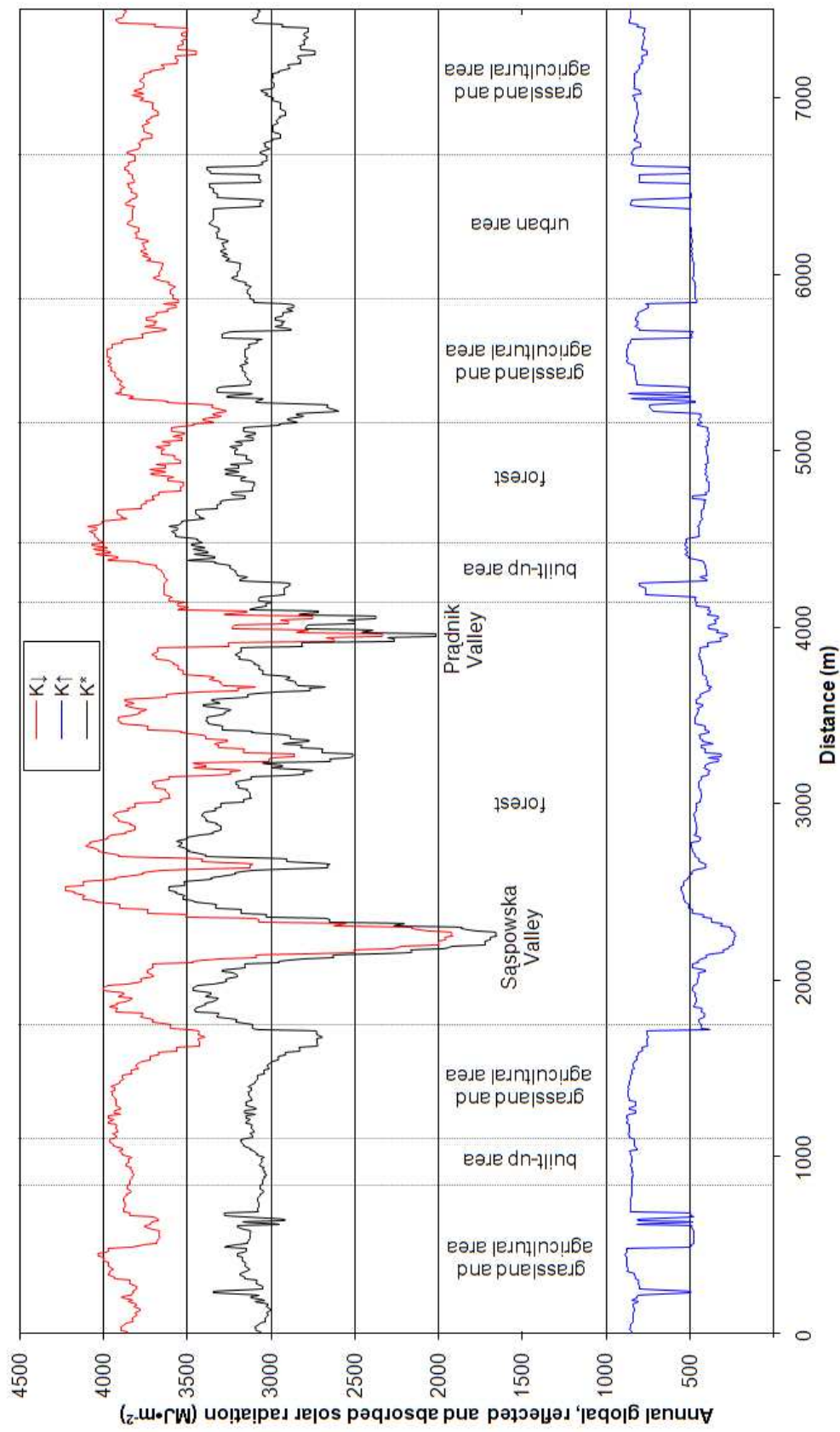


Fig. 7. Course of annual global  $K_{\downarrow}$ , reflected  $K_{\uparrow}$  and absorbed  $K^*$  solar radiation in profile SW-NE